PAN POLSKA AKADEMIA NAUK

METROLOGY AND MEASUREMENT SYSTEMS

Index 330930, ISSN 0860-8229
www.metrology.pg.gda.pl

M&MS

MEASUREMENT OF THE UPPER RESPIRATORY TRACT AERATED SPACE VOLUME USING THE RESULTS OF COMPUTED TOMOGRAPHY

Adam Rybak[1)], Andrzej Zając[1)], Andrzej Kukwa[2)]

1) *Military University of Technology, Institute of Optoelectronics, Gen. W. Urbanowicza 2, 00-908 Warsaw, Poland* (*adam.rybak@wat.edu.pl*, ✉ *andrzej.zajac@wat.edu.pl*, +48 48 261 837 398)
2) *University of Warmia and Mazury, Department of Otolaryngology and Head and Neck Disease, Warszawska 30,10-832 Olsztyn, Poland* (*g_andrzejkukwa41@gmail.com*)

Abstract

The paper presents the possibilities of quantitative analysis of results obtained from CT examination of organs and anatomical structures of the upper respiratory tract. The presented results of the analysis were obtained using proprietary software developed in the MATLAB 2018b environment (Image Processing toolbox). The software enables to visualize the original results of CT scan and, after evaluating the visible structures, enables to select the area to be subjected to quantitative analysis. After the initial identification of an area of interest requiring detailed diagnostics, its volume and the surface areas of individual cross-sections are calculated in the area separated for examinations. A graphical presentation of the analysis results – the surface areas of selected cross-sections possible to visualize in two- and three-dimensional space – enables quick analysis of changes in the examined region.

Keywords: CT studies, upper respiratory tract diagnostics, quantitative measurement of upper respiratory tract aerated space volume.

1. Introduction

Diagnostics using the methods of spatial imaging of biological structures in *Computed Tomography* (CT) has been used in clinics since 1971, *i.e.* for 48 years. The method itself was developed earlier – in 1956, and Ronald Bracewell used this method to develop solar maps. The first devices that Radon's ideas were tried to adopt in were constructed in 1961 by William H. Oldendorf, in 1963 by Allan MacLeod Cormack from Tufts University, and in 1968 by David Kuhl and Roy Edwards. They all contributed to the final result achieved by Godfrey N. Hounsfield, who was the first one to develop a functioning diagnostic system and presented its unique capabilities. Hounsfield and Cormack received the 1979 Nobel Prize for the invention and construction of a computed tomography scanner [1].

The first tomography scanner was installed in the Atkinson Morley Hospital in Wimbledon, London. The first patient was examined there in 1971. In the United States, it was sold at a price of 390,000 USD at that time, and the first CT scanners were installed in 1973 in Mayo Clinic and Massachusetts General Hospital. The methodology of examinations using CT constantly evolves.

Article history: received on Mar. 15, 2019; accepted on Mar. 30, 2019; available online on Jun. 28, 2019, DOI: 10.24425/mms.2019.128366.

In the old methodology of tomography, images were obtained in the transverse plane – the device irradiated the body of the examined person, which was then reproduced on X-ray film, followed by moving the examined body and the procedure was repeated. The following CT systems are currently available [2]:

- *Multi-Slice Computed Tomography* (MSCT, *Multi-row-Detector Computed Tomography*, MDCT) – a technique introduced into medical diagnostics in 1998, based on CT technology with a much greater number of elements enabling to develop imaging – an image. The first MDCT systems introduced in 1998 offered simultaneous acquisition of signals from four rows of detectors with a single detector row width of 1 or 1.25 mm with a rotation time of up to 0.5 seconds. The first MDCT systems made it possible to shorten the study time, but did not improve the spatial resolution. Only 16-row CT systems introduced in 2001 allowed to reduce the spatial resolution to 0.5 mm. In 2007, a CT scanner with a collimation of 320×0.5 mm, covering 16 cm in an isocentre with a gantry rotation time of 0,35 s [3–10] was launched on the market. Clinical experience with 64-, 128- or 256-row CT equipment indicates that the MDCT performance has reached a level close to the maximum of technical capabilities, and simply adding even more rows of detectors will not result in increased clinical benefits [3].
- A method using 2 X-ray tubes for examination – enables to reduce the examination time, reduce the radiation dose and at the same time to obtain much more data, *i.e.* more accurate imaging of the examined organs. The method using 2 X-ray tubes resulted in technical difficulties associated with an increasing number of detector rows. The simplest solution for manufacturers was to construct a "new" two-tube scanner from two "older" single-tube scanners. The main challenge for a dual-source CT system is diffuse radiation, *i.e.* radiation from X-ray tube B detected by detector A and *vice versa*. Diffuse radiation can produce artefacts if it is not corrected. Dual-source CT systems exhibit interesting properties also for general radiological applications. Both X-ray tubes can be used at different values of the tube's electrical field and current in the system to differentiate the obtained images. The use of a dual-tube CT scanner can substantially increase the amount of morphological information obtained [3].

In the new multi-row CT scanners, the data are digitally recorded continuously, as these scanners provide a so-called spiral volumetric scan. They can then be reconstructed using the following graphic techniques [2]:

- MIP (*maximum intensity projection*) – projection of the highest intensities, used in the imaging of blood vessels.
- MPR (*multiplanar reformated reconstruction*) – reconstruction in any plane, enabling to assess the cross-sections of vessels, the myocardium, and heart valves.
- VR (*volume rendering*) – volumetric reconstruction, enabling to obtain three-dimensional images to reproduce anatomical relations, for example, the vascular pattern.
- SSD (*shaded surface display*) - surface reconstructions in which an image is created from the surface pixels with the highest degree of absorption.

All the aforementioned devices and reconstruction techniques are mostly related to qualitative diagnostics – the radiologist describes the obtained tomogram, specifying the morphological changes observed in the diagnosed patient.

Quantitative analysis in a significant part of cases boils down to the evaluation of local lesions in the diagnosed area, including examinations with administering a contrast agent. Objective quantitative measurements, including cases of more extensive lesions, are a relatively rare case in clinical practice.

2. Analysis of problems during measurement of empty space volume within upper respiratory tract

Hypoxia – primary being not painful – brings about and even promotes the degradation of: cells, tissues, organs, including the entire body, following the resulting complications that develop. The sensation of "stuffy/obstructed nose" is perceived in almost 30% of the adult population, therefore it is a frequently observed and reported ailment. It is due to various degree of impaired airway patency, and thus impaired airflow through the nasal cavity and other parts/sections of the upper respiratory tract. It should be added that the most important reason for this condition is the different degree of increase in respiratory resistance, which is an indicator of impaired patency.

The pathomechanism of obstruction resulting from impaired breathing within the upper respiratory tract is multifactorial. However, anatomical changes of the bones and the soft parts of the facial skeleton are most often considered to be the cause. The aforementioned anatomical changes, as indicated, develop on the basis of deformations in the skeleton and the soft parts of the upper respiratory tract. In particular, they result from: hypertrophy of lymphatic tissue in the nasal and oral parts of the throat, as well as muscles and mucous membrane.

However, the state of impaired patency is perceived in various ways and reported in the form of patients' complaints as a disease symptom in different conditions and periods. The nose and the nasal sinuses forming an inseparable entirety with it, constitute a complex of anatomically complicated ducts and air spaces. This system performs very important physiological functions affecting physical parameters and the composition of inhaled and exhaled air.

It seems that many functions and their mechanisms in the nasal cavities and the paranasal sinuses are still not sufficiently studied. The authors are convinced that the development and implementation of innovative measurement methods into clinical practice, with the use of which it will be possible to properly assess the condition of cavities and air canals within the upper respiratory tract, will support the phase of diagnostics both before and after the application of a selected treatment and will facilitate optional verification of therapeutic proceedings. The last problem in particular should enable to use quantitative analysis of the upper respiratory tract geometry. Accurate quantitative analysis of parameters of canals and cavities within the upper respiratory tract region will significantly improve diagnostics in this area, and capture possible slow-changing repair processes in the post-surgical period.

Currently, using software methods for this purpose is not possible on a larger scale. Generally available commercial programs for quantitative analysis are usually closely associated with the software created for a specific manufacturer's equipment. The known literature reports and available information on software from CT equipment manufacturers – *e.g.* General Electric [11] or Medixant [12] – show that the available commercial software does not include ready-made algorithms dedicated to quantitative analysis of parameters of air ducts within the upper respiratory tract. This problem also concerns the quantitative evaluation of the volume parameters of sinus cavities. Such a situation in many cases results in limitations of quick hospital diagnostics, including comparing the effects of therapy and the results of surgical treatment. This is particularly important in clinical practice and in the evaluation of the study results by the staff directly in the department.

Measuring the volume of upper respiratory tract aerated space – *e.g.* of the aerated space of paranasal sinuses or bronchial tree in the lungs – using currently available software is not intuitive, and the obtained reconstructions are not always readable enough. To support the process of quantitative CT diagnostics within the upper respiratory tract, a solution dedicated to the analysis of patients' air ducts based on standard CT examination was developed. Our proprietary software enables a quick reconstruction of multi-row CT and conical CT tests saved in DICOM format.

The software is adapted to quantitative analysis of air structures registered in a CT scan. Compared with the known commercial software supplied to the General Electric CT scan impression station ("AW Volume Viewer") [11] or the paid version of Medixant's RadiAnt software [12], the accuracy of the obtained results – concerning *e.g.* sinuses and the air waist in the upper respiratory tracts – is higher. The obtained accuracy enables to reproduce and quantitatively analyse even small aerated spaces – with the size of a step-by-step recording of CT results. One of the commercially available programs with the application similar to the one developed by the authors of the software is Materialise's Mimics [13], which enables, among other things, qualitative analysis of selected areas of CT scan, *e.g.* sinuses. It calculates the volume and includes an automatic function of detecting the entire sinus. The program works well in the case of qualitative, not quantitative analysis, because it shows the shape of the object in three dimensions. It does not illustrate the interior of the sinus in a simple way for analysis and does not show the change in sinuses, *e.g.* an area of individual dimensions. The software is widely used for various medical and non-medical applications. The software has a rich user interface, which is due to a wide range of applications of the software, because each of them brings additional functions to the software. Because of that, the software requires training and is less intuitive to use than a program that is applied only to the sinuses. In addition, the program does not allow interference with the sinus' marginal area, which is not clearly defined in the area of CT scan. The program contains several methods of segmentation, *i.e.* basic – automatic and other semi-automatic methods. Each of these methods is characterized by better performance in different applications. The manufacturer recommends using automatic segmentation and, if the results are unsatisfactory, using other available methods. Fig. 1 shows the user interface of Materialise's Mimics software.

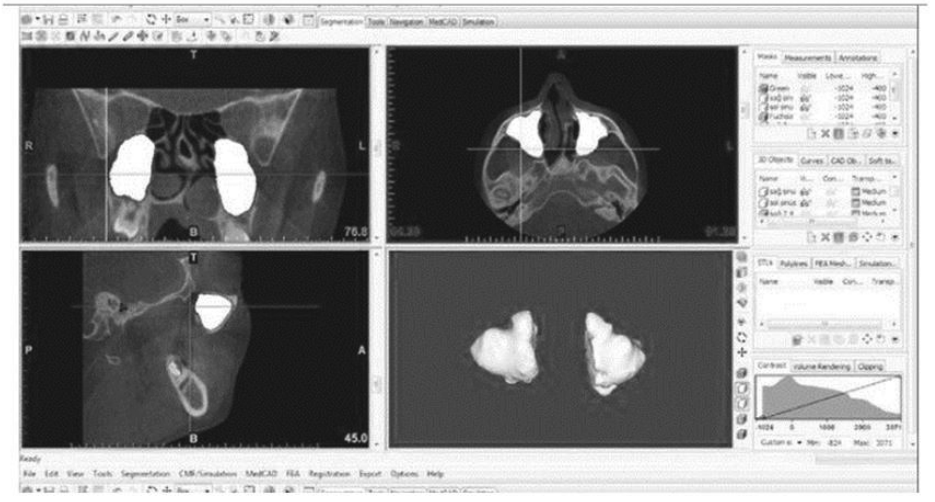

Fig. 1. The user interface in the Mimics software from Materialise [14].

3. Segmentation as way of organizing information extracted from CT test results

CT results contain information about the absorption of radiation by the tested objects located in the CT examination area. In order to simplify the interpretation of CT results, it is required to exchange information about the absorption of the media through which it passes to the components of the object. The obtained information is limited to displaying only the necessary data

(*e.g.* specific tissues) for detailed diagnostics of the examined object, *i.e.* calculation of its volume. Segmentation is a tool used to specify interesting information from an image containing a large number of details obscuring the region of interest. An example of the use of segmentation includes the brain scan, during which it would not be possible to divide the examined image into different areas differentiated by the greyscale without the use of segmentation. Thanks to such a procedure, it is possible to identify active areas of the brain, *e.g.* during stimulation with selected stimuli [20, 21]. Image segmentation is one of the most important parts of image processing.

The methods of image segmentation can be divided into:

– Region growing methods – the region is composed of adjacent pixels and the boundary is the grey-level difference between the regions. There are two methods of segmentation by region growing: greyscale thresholding and region enlargement [22–24].
  Greyscale thresholding is based on the assumption that images are created from regions with different greyscale levels. A shading level histogram of the analysed region contains a quantitative set of occupation for individual fragments of the image with the same optical density. The threshold is a value on the histogram that decides to which group, due to its intensity level, a pixel will be assigned. The first group – "first plan", shall include pixels with an intensity level greater than or equal to the threshold value, and the second group – "background", shall include pixels below the threshold value. Thanks to the use of more than one threshold, it is possible to separately create more objects with different greyscale thresholds [25–27].
  The result of the greyscale-level thresholding method is a number of separated regions in the image. In order to separate one region and remove the other ones, segmentation with the region growing method by region enlargement is used – a pixel must both meet the criterion of intensity and belong to the vicinity of the pixel that has been included in a specific region. If the same objects, *e.g.* tissues, do not come into contact, they shall be separated. There is a risk that areas characterized by highly variable intensity values will not be separated. This method has two input parameters: the starting point of the initial object and the criterion for attaching new pixels [28–30].
– A classification method – consists in searching for a pattern in the data. Classification is a technique which searches for and recognizes patterns using data. Reference data contain a sample of graphic elements together with information about their purpose. This is a learning technique, because first the data are divided into segments manually and then they are replaced by an automatic process [31, 32].
– A cluster method – consists in grouping pixels into relatively homogeneous classes, in which pixels are more closely related to each other than pixels grouped in other classes. In most algorithms, the basis for grouping is the similarity between elements expressed by the function (metrics) of similarity. Grouping consists in separating groups (classes, subsets). The most popular clustering algorithms are:
  • the k-means method, in which grouping is based on the initial division of the population into a predetermined number of classes (so-called clusters);
  • the fuzzy clustering analysis method, the fuzzy – c-means method, in which elements can be allocated to more than one category;
  • the expectation maximization method, in which the probability of belonging to clusters is calculated assuming one or more probability distributions.
– A hybrid method – is a combination of several of the mentioned methods of segmentation [19, 35].

The choice of a segmentation method is not always obvious due to the different features of the tested objects, *e.g.* the differences in radiation absorption in the surrounding tissues resulting

in a complex relation of the optical density of the analysed pixel to the areas lying in the path of the beam. Consequently, there is no single, effective segmentation method that is universal and has a wide range of applications. Two solutions are known to this problem. The first one consists in including several methods of segmentation in the software and leaving the method selection to the user. However, using this solution is complicated and burdened with a human error. An alternative to this solution is to develop an application dedicated only to specific areas of interest, with specific properties. Thanks to this, the risk of selecting a wrong method is eliminated, and the obtained results are consistent, regardless of the application's user. Such a solution can be optimized, since it requires less computing power and can be more intuitive to use [15–18].

The aforementioned reasons lead to a situation that currently on the market there are no solutions applicable only to the measurement of the upper airway aerated space volume using CT scans. The software currently available on the market is only part of a larger software and is not intended for narrow applications only. It was decided to fill this niche on the market with a proprietary software applied to the diagnostics of the upper airway aerated spaces.

The developed program is mainly based on segmentation of CT scan results. The proprietary software is used for quantitative diagnosis of volume in the upper respiratory tract space. The results of a standard CT scan are used to obtain these data. In order to separate the area, it uses two methods of segmentation by region growing, *i.e.* greyscale-level thresholding and region enlargement ones. First of all, the program performs the grey-level thresholding. The result of the thresholding is a number of isolated regions in the image. Next, in order to separate one region and remove the other ones, the program uses the region growing method of segmentation. This segmentation method was selected having on mind optimization of the program's performance in terms of the necessary computing power – time of calculations for one case of analysis.

4. Method of analysing image obtained by computed tomography

Using the program, it is possible to preview the results of CT scan reconstruction of the region in order to select the limited region to be analysed. Narrowing the area of interest is feasible thanks to the functionality developed in the graphical user interface. The user can isolate a specific fragment, *e.g.* a sinus, by means of segmentation, from a narrowed region.

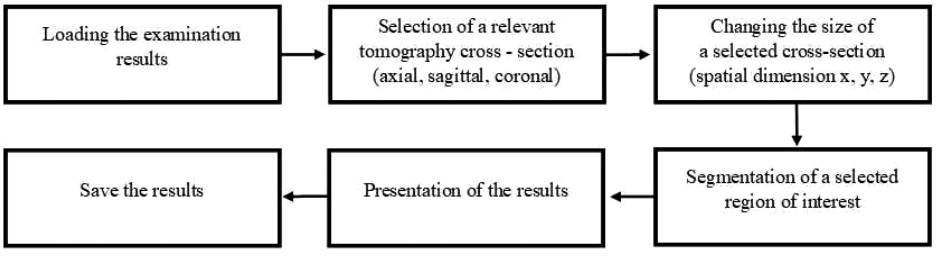

Fig. 2. A block diagram of the image analysis method results obtained from a CT scan.

The main elements of the program for CT analysis are:

– loading the examination results, selection of a relevant tomographic cross-section (axial, sagittal, coronal);
– changing the size of a selected cross-section (spatial dimension x, y, z);

– segmentation of a selected region of interest and presentation of the results, *e.g.* in the form of diagrams, and saving them.

Each of the successive steps is essential for the entire CT scan analysis method, and the individual steps are interlinked.

A detailed diagram of the program operation is shown in Fig. 3. Installation of the program is very simple and intuitive. Two components are installed on the user's computer. These include the described program and, if needed, the libraries necessary to run the program.

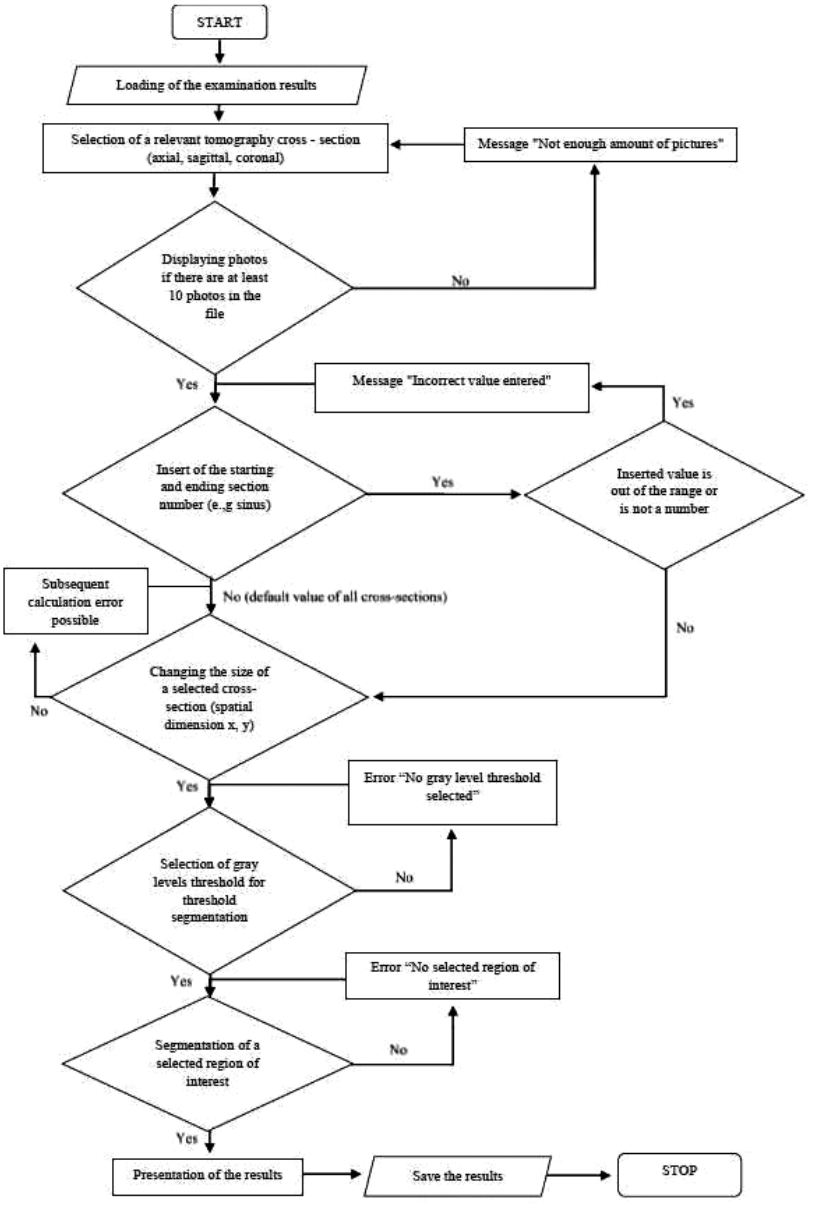

Fig. 3. A detailed block diagram of the CT analysis method.

4.1. Loading of test results

The program enables to load a scan stored in DICOM standard, typical for CT tests. This recording standard has been chosen due to its common use in commercial CT equipment and the ability to record scans in this standard on majority of devices, as well as no restrictive copyright for the software that uses this standard. As far as the software is concerned, it does not matter what data carrier the test results are saved on. The user is asked only to indicate a relevant directory, and the software loads only those directories in which there are at least 10 images.

4.2. Selection of relevant tomography cross-section

Due to the lack of a standard in the description of CT scans performed by radiologist technicians, it is required to indicate a tomographic cross-section being the object of the scan. The program has the ability to preview each tomographic cross-section also during its selection. It is then possible to preview the selected cross-section at each image processing stage.

4.3. Changing size of selected section (spatial dimension x, y, z)

After selecting an interesting CT cross-section, most of the cross-section area is an image outside the region of interest. In order to save memory space and speed up calculations, the user shall select a specific region of interest from the original image. In the first stage, two layer numbers are entered, on which the region of interest begins and ends. Then, using two sliders, the user shall limit the dimensions of the image on X and Y axes.

4.4. Segmentation of selected region of interest and presentation of results

The program automatically selects the black threshold for segmentation using the threshold method, and displays a preview of the image. Due to the limitation of the automatic algorithm to one layer of the image, the application requires the user to select a threshold for the greyscale level using a slider. The grey-level area of a specific image pixel is one of the criteria for homogeneity. The result of segmentation is a binary image, in which the pixels for the user-defined value are 0, and above them, they take the value of 1. The result is several regions of interest with the same pixel value.

Separation of a specific region from the others is done next by means of the region growing method of segmentation by region enlargement. In order to do so, the program requires the cursor to indicate the region of interest in the image. Using the area expansion segmentation method, one can define moving curves in the image to find the boundaries of the object. This segmentation is an iterative method that uses 200 repetitions of operations to precisely determine the area. For faster and more accurate segmentation results, the user specifies an initial contour position in each section that is close to the required object boundaries.

In the next step, the specified area is calculated for each section and its volume. The results are presented in the *Information* section of the program as well as in two-dimensional and three-dimensional space diagrams presented in Fig. 4. A graph in a two-dimensional space shows the change in the surface area of the cross-sectional area. The example is illustrated in Fig. 5.

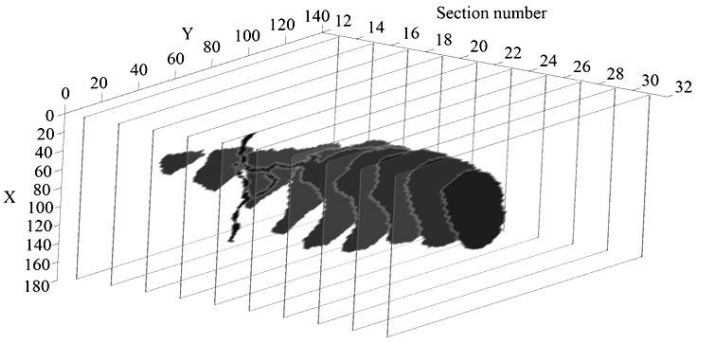

Fig. 4. An example illustrating the spatial structure of examined sinus. On X axis, the horizontal dimension of the sinus is indicated, on Y axis – the vertical dimension of the sinus. The given sinus area is marked in dark colours.

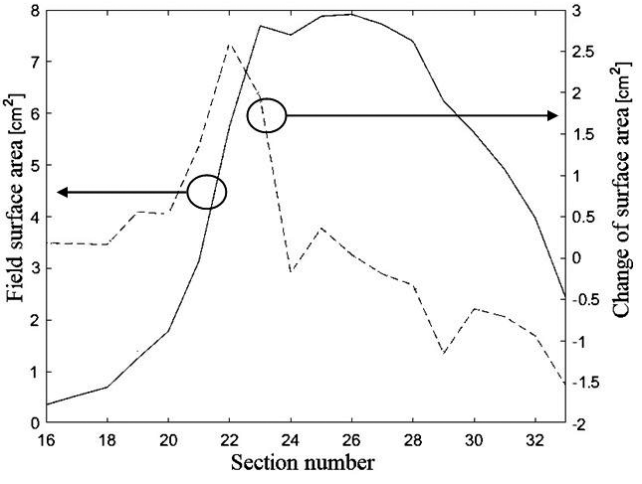

Fig. 5. A surface area for the region interest for individual cross-sections.

4.5. Saving results

The program enables to save the work results in any location. The format of saved results is a significant facilitation for the operator, as it is the most versatile, and at the same time economical, in terms of data volume. Images and charts are saved in one of the most common formats – *.JPEG format (very often used in computer graphics), and all numerical data are saved in the *.xls format (Microsoft Excel software). The use of standard formats will make it easier to view them later on any computer without the need of cumbersome installation of software on it.

5. Program for quantitative analysis of CT scan

The program was developed in Matlab 2018b environment using the Image Processing toolbox. A *graphical user interface* (GUI) is used to control the program. In order to simplify the program's operation, the main program window has been divided into sections. Each section is

responsible for a certain stage of the program's operation. The first section, from which the user starts operating the program, is called *Beginning*. It is shown in Fig. 7.

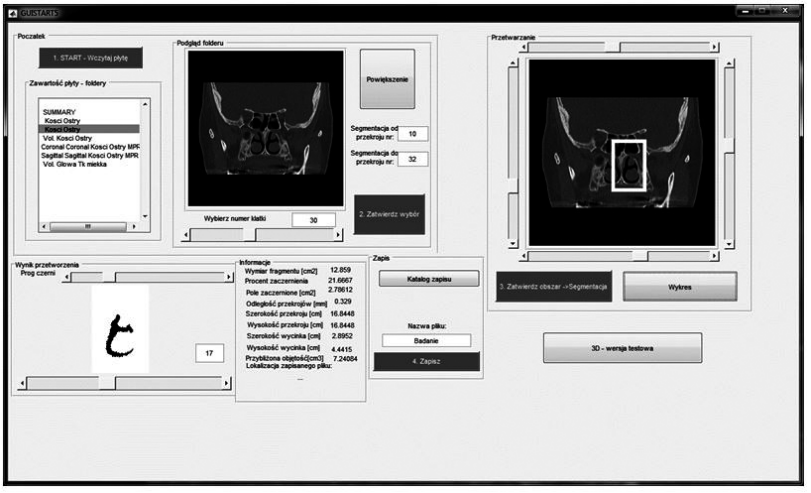

Fig. 6. The main window of the software.

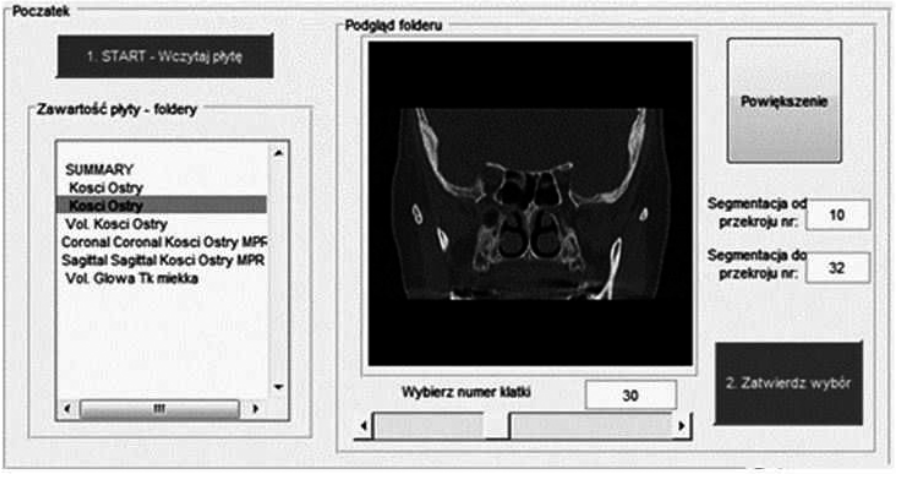

Fig. 7. The first section *Beginning* in the main window of the software.

The operation of this section is very intuitive. The main buttons used for operation are highlighted in blue. In case a user executes an incorrect command, an error message is displayed. The *Beginning* section has been extended by an additional window, which is called up using the *Zoom* button. The new window enables to preview photos in an enlarged format, so that the image is even more readable. After the preview is finished, the user returns to the main part of the program. The *Processing* section is responsible for narrowing the area to be analysed and then selecting a specific region of interest. The *Processing Results* section enables to preview the image after processing. Additionally, in the *Information* section, there is provided the basic

information necessary during the work, *i.e.*: the surface area of the selected fragment, or the cross-section or specimen size. The last section, called *Recording*, is responsible for saving the results of the program's work.

6. Calculation results and uncertainty of measurement

The program can calculate the surface area of a selected tomographic cross-section after changing its size, darkness percentage, the surface area of a selected region of interest after applying segmentation for selected tomographic cross-sections, and the surface area of a selected region of interest. An important element of any software is the verification of correctness and the estimation of accuracy of its operation. The proprietary software has been tested in a limited number of cases and compared with statistical data for the calculated areas. For the elements of the program related to the calculation uncertainty, an estimation error has been calculated.

In order to calculate the volume of a selected region of interest (*e.g.* a sinus), its surface areas for individual cross-sections are calculated first. Due to the lack of access to statistical data on the surface area (*e.g.* sinus), the volume data were used to verify the operation of the program.

The results of the program for a sample of 10 patients showed that the calculation of sinus volume is close to the mean statistical sinus volume – the results for the selected four patients are presented in Table 1. For two of them we can observe pathologies. Fig. 8 shows a typical result of the program demonstrating a change in the surface area of the selected region of interest. One of the main errors in the calculation of the surface area and the volume in the upper respiratory tract, *e.g.* a sinus, by the program, is the error caused by ambiguous determination of its borders. A tissue between the sinus and the bone tissue often makes it difficult to define the boundaries of

Table 1. An example of calculated sinus volume for four patients.

Patient	Measured element	Volume [cm^3]
1.	left sinus	23.9467
	right sinus	23.8408
2.	left sinus	19.2322
	right sinus	19.0019
3.	left sinus	16.6408
	right sinus	25.8388
4.	left sinus	32.4459
	right sinus	19.2153

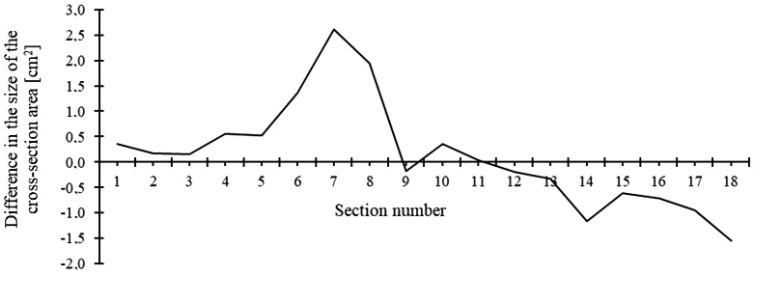

Fig. 8. The main window of the software.

the sinus. This tissue may include *e.g.* an area with inflammation. In the program, the user uses the slider to define the greyscale-level threshold, *i.e.* the border between inflammation and the sinus. This estimation gives rise to an estimation error. It has been calculated for two extreme cases – the first for a minimum acceptable greyscale-level threshold and the second for a maximum acceptable greyscale-level threshold. The estimation error for the different estimations of the sinus boundaries was about 3%. Calculation of the sinus volume for every second frame of CT recording increases the error by +/ − 1%. An example of the error calculation for the case of calculating the spatial parameters of sinuses using each second frame of the CT scan is shown in Table 2 and Figs. 8 and 9.

Table 2. Calculated estimation errors for the sinus volume when counting every second frame.

Measured element	**Volume [cm^3]**	**Volume – calculated every second frame starting from odd one [cm^3]**	**Volume – calculated every second frame starting from even [cm^3]**	**Estimation error – calculated every second frame [%]**	**The maximum estimation error [%]**
left sinus	37.96264	37.74819	38.17709	+/ − 1%	5%
right sinus	27.00065	27.25807	26.74322	+/ − 0.6%	4.2%

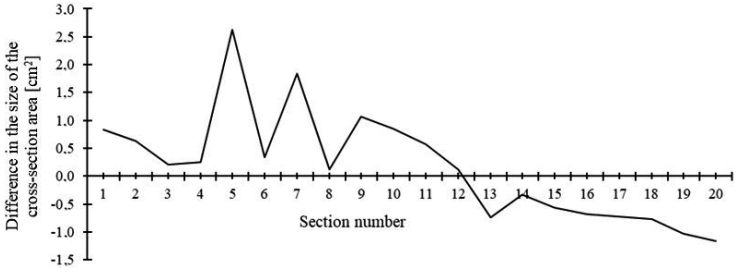

Fig. 9. The first section *Beginning* in the main window of the software.

Taking into account the foregoing considerations, it can be assumed that the maximum estimation uncertainty for the area size of a sinus cross-section resulting from the user taking the cut-off threshold value in the greyscale and changing the start point during segmentation is 5%. Calculations of the sinus volume made for every second section of the CT scan indicate that the gradient of changes in the size of the aerated space in the examined structure does not introduce additional significant changes in the measurement level of uncertainty.

7. Conclusions

According to the authors' knowledge, there are currently no products dedicated to quantitative measurements of the aerated space in the upper respiratory tract available on the market. In the presented material, we indicate this possibility using typical CT scan results of patients. We believe that the software presented in the paper may fill the existing niche on the market. The program has been developed and tested on selected CT scan results of patients treated for various upper respiratory tract diseases in Department of Otolaryngology and Head and Neck Disease, University of Varmia and Mazury, Warszawska st. 30, Olsztyn.

The program's operation is essentially based on the segmentation of CT scan results and is a tool for the diagnostics of upper airway aerated space. In order to separate the area of a selected anatomical region, the program uses two methods, *i.e.* grayscale level thresholding and region enlargement, of segmentation by region growing.

The developed program enables to preview the results of a CT scan saved in DICOM format. The application accelerates the analysis of the condition and functionality of the upper respiratory tract, in particular the spatial evaluation of sinuses and canals, by applying the method of segmentation providing optimal results.

The program has implemented the 3D visualization feature developed for the needs of visualization of complex anatomical structures of upper respiratory tract. An example of the analysis results obtained with the developed software for selected upper respiratory tract structures is presented in Fig. 4. Thanks to the intuitive and simple user interface dedicated to the region of application in the analysis of the upper respiratory tract structures, the program's operation is not time-consuming.

The developed software was tested on a selected group of patients, and the results obtained for the analysed upper respiratory tract aerated areas were compared with the literature data. The obtained calculation results are consistent with expectations, and their statistical analysis indicates that there is sufficient consistency with the population data. The resulted uncertainty is satisfactory and is equal to about 5%. It can therefore be concluded that the adopted test methodology, developed numerical procedures for CT imaging analysis and, as a result, the entire developed program operate properly.

Competitive applications work well in the case of qualitative, not quantitative analysis, as they show the shape of an object in three dimensions which enables only a general evaluation of the lesion. They do not illustrate the interior of *e.g.* sinus in a simple way for analysis and do not show the change in sinuses, *e.g.* the surface area of individual dimensions. Compared with the solutions available on the market, the developed software is characterized by a narrow application targeted at diagnosing the upper respiratory tract. The developed application is intuitive and enables faster analysis of results. In addition, the program includes a unique method of presenting the results, which enables to compare changes in the cross-sectional area.

The nose and the nasal sinuses forming an inseparable entirety with it, constitute a complex of anatomically complicated ducts and air spaces. This system performs very important physiological functions affecting physical parameters and the composition of inhaled and exhaled air. It seems that many functions and their mechanisms in the nasal cavities and the paranasal sinuses are still not sufficiently studied. The developed software provides a more precise, quick and quantitative means of diagnostics of the upper respiratory tract.

References

[1] Pietzsch, J. (2017). *The Nobel Prize in Physiology or Medicine 1979*. Allan M. Cormack, Godfrey N. Hounsfield, Perspectives.

[2] Walecki, J., Zawadzki, M. (2006). Postępy w diagnostyce obrazowej w 2005 roku. *Medycyna praktyczna*, 7(8), 185–186.

[3] Flohr, T. (2013). *Current Radiology Reports*. 1(1), 52–63.

[4] Klingenbeck-Regn, K., Schaller, S., Flohr, T. (1999). Subsecond multi-slice computed tomography: basics and applications. *European Journal of Radiology*, 3(12), 110–124.

[5] McCollough, C.H., Zink, F.E. (1999). Performance evaluation of a multi-slice CT system. *Med. Phys.*, 26(11), 2223–2230.

[6] Hu, H., He, H.D., Foley, W.D., Fox, S.H. (2000). Four multidetector-row helical CT: image quality and volume coverage speed. *Radiology*, 215(1), 55–62.

[7] Mori, S., Endo, M., Tsunoo, T., Susumu, K., Tanada, S., Aradate, H. (2004). Physical performance evaluation of a 256-slice CT-scanner for four-dimensional imaging. *Med. Phys.*, 31(6), 1348–1356.

[8] Mori, S., Endo, M., Obata, T., Tsunoo, T., Susumu, K., Tanada, S. (2006). Properties of the prototype 256-row (cone beam) CT scanner. *European Radiology*, 16(9), 2100–2108.

[9] Mori, S., Kondo, C., Suzuki, N., Hattori, A., Kusakabe, M., Endo, M. (2006). Volumetric coronary angiography using the 256-detector row computed tomography scanner: comparison in vivo and in vitro with porcine models. *Acta Radiology*, 47(2), 186–191.

[10] Kido, T., Kurata, A., Higashino, H., Sugawara, Y., Okayama, H., Higaki, J., Anno, H., Katada, K., Mori, S., Tanada, S., Endo, M., Mochizuki, T. (2007). Cardiac imaging using 256-detector row four-dimensional CT: preliminary clinical report. *Radiation Medicine*, 25(1), 38–44.

[11] AW Volume Viewer. *https://www.gehealthcare.com/en/products/advanced-visualization/all-applications/volume-viewer*. (2019).

[12] RadiAnt. *https://www.radiantviewer.com/pl/*. (2019).

[13] Mimics. *https://www.materialise.com/en/medical/software/mimics*. (2019).

[14] Agacayak, K.S., Gulsun, B., Koparal, M., Atalay, Y., Aksoy, O., Adıgüzel, Ö. (2015). Alterations in Maxillary Sinus Volume among Oral and Nasal Breathers. *Medical science monitor*, 21, 18–26.

[15] Hassan, E., Aboshgifa, A. (2015). Detecting Brain Tumour from Mri Image Using Matlab GUI Programme. *International Journal of Computer Science & Engineering Survey*, 6(6), 47–60.

[16] Chu, C., Takaya, K. (1993). 3-Dimensional rendering of MR images. *WESCANEX 93. Communications, Computers and Power in the Modern Environment Conference Proceedings*, IEEE,165–170.

[17] Clarke, L., Velthuizen, R., Camacho, M., Heine, J., Vaydianathan, M., Hall, L., Thatcher, R., Silbiger, M. (1995). MRI segmentation: Methods and applications. *Magnetic Resonance Imaging*, 13, 343–368.

[18] Leemput, K.V., Maes, F., Vandermeulen, D., Suetens, P. (1999). Automated model-based tissue classification of MR images of the brain. *IEEE Trans. on Medical Imaging*, 897–908.

[19] Norouzi, A., Shafry, M., Rahim, M., Altameem, A., Saba, T., Ehsani Rad, A., Rehman, A., Uddin, M. (2014). Medical Image Segmentation Methods, Algorithms, and Applications. *IETE Technical Review*, 31(3), 199–213.

[20] Lim, K., Pfefferbaum, A. (1989). Segmentation of MR Brain Images into Cerebrospinal Fluid Spaces, White and Gray matter. *Journal of Computer Assisted Tomography*, 13(4), 588–593.

[21] Lucas-Quesada, F.A., Sinha, U., Sinha, S. (1996). Segmentation strategies for breast tumors from dynamic MR images. *J. Magn. Reson. Imaging*, 6(5), 753–763.

[22] Davies, E. (2005). *Machine Vision: Theory, Algorithms, Practicalities*. San Francisco, CA: Morgan Kaufmann.

[23] Sonka, M., Hlavac, V., Boyle, R. (1999). *Image processing analysis and machine vision*. 2nd ed. Pacific Grove, CA: PWS Publishing, 123–133.

[24] Norouzi, A., Rahman, A., Shafry, M., Saba, T. (2012). Visualization and segmentation. *Int. J. Acad. Res.*, 4(2), 202–208.

[25] Dalvi, R., Abugharbieh, R., Wilson, D., Wilson, D.R. (2007). Multi-contrast MR for enhanced bone imaging and segmentation. *Conf. Proc. IEEE Eng. Med. Biol. Soc.*, 5620–5623.

[26] Rad, E.A., Rahim, M.S.M., Rehman, A., Altameem, A., Saba, T. (2013). Evaluation of Current Dental Radiographs Segmentation Approaches in Computer-aided Applications. *IETE Tech. Rev.*, 30(3), 210–222.

[27] Pham, D.L., Xu, C., Prince, J.L. (1998). A Survey of Current Methods in Medical Image Segmentation. *Ann. Rev. Biomed. Eng.*, 2, 315–337.

[28] Nguyen, N., Laurendeau, D., Branzan-Albu, A. (2007). A new segmentation method for MRI images of the shoulder joint. *Fourth Canadian IEEE Conference on Computer and Robot Vision (CRV'07)*, Montreal, 329–338.

[29] Kallergi, M., Woodsa, K., Clarkea, L., Qiana, W. (1992). Image segmentation in digital mammography: Comparison of local thresholding and region growing algorithms. *Computerized Medical Imaging and Graphics*, 16(5), 323–331.

[30] Olivera, A., Freixeneta, J., Martia, J., Pérezb, E., Pontb, J., Dentonc, E., Zwiggelaard, R. (2010). A review of automatic mass detection and segmentation in mammographic images. *Med. Image Anal.*, 14(2), 87–110.

[31] Bishop, C.M. (2006). *Pattern Recognition and Machine Learning. Springer*, 1–5.

[32] Theodoridis, S., Pikrakis, A., Koutroumbas, K., Cavouras, D. (2010). *Introduction to Pattern Recognition: A Matlab Approach. Burlington*. VT: Academic Press.

[33] Wells, W. Grimson, W., Kikins, R., Jolesz, F. (1996). Adaptive segmentation of MRI data. *IEEE Trans. Med. Imag.*, 15(4), 429–442.

[34] Mantas, J. (1987). Methodologies in pattern recognition and image analysis – A brief survey. *Pattern Recognition*, 22(1), 1–6.

[35] Ababneh, S.Y., Prescott, J.W., Gurcan, M.N. (2011). Automatic graph-cut based segmentation of bones from knee magnetic resonance images for osteoarthritis research. *Med. Image Anal.*, 15(4), 438–448.